13th World Conference on Earthquake Engineering
Vancouver, B.C., Canada
August 1-6, 2004
Paper No. 2191

Fire Following Earthquake Loss Estimation

Christian P. Mortgat[1], Abdel Zaghw[2] and Ajay Singhal[3]

SUMMARY

Fire following earthquakes can cause significant losses that, at times, have exceeded earthquake shake losses. Due to the complexity of conflagration modeling, simulation techniques are used to provide estimates of the potential fire losses under earthquake scenarios. This paper describes the simulation technique and its components. Results for selected scenario events in the United States are presented.

INTRODUCTION

Fire following earthquake (FFEQ) has the potential for generating significant damage. The conflagration fires following the 1906 San Francisco earthquake significantly exceeded the shake losses and resulted in the largest earthquake loss in American history. Similarly in Japan, the fire losses following the 1923 Great Kanto earthquake were much larger than the shake losses. Surprisingly in the United States, contrarily to Japan, little research is done on the topic. However, future loss estimators would be useful for urban planners and insurance companies as demonstrated by the recent Northridge earthquake (1994) where the fire losses amounted to about $500M.

This paper presents the components of a methodology and the associated implementation tool developed to estimate FFEQ losses. Some of the components were originally developed for Japan. They were modified and adapted to the U.S. environment. Due to the complexity of conflagration modeling, time-step simulations are necessary to reasonably quantify the phenomenon. The simulation is performed for a selected region and a specific scenario earthquake. The progression of the fires is followed from ignition to control or burn out at each step of the simulation. At the end of the simulation, the burnt area is recorded. The loss is determined by overlaying the exposure over the burnt area. The simulation is repeated many times for the same region and the same event while letting the uncertain parameters vary according to their distributions. At the end of a series of simulations, the mean loss and the corresponding coefficient of variation are determined for the region. The uncertainty associated with fire losses is therefore captured and quantified. Selected random parameters can also be fixed (such as wind speed or time of occurrence of the event) to assess the sensitivity of the results to those parameters.

[1] Vice President, Risk Management Solutions, Inc. 7015 Gateway Blvd, Newark, CA 94560
[2] Associate Professor, Structural Engineering Department, Cairo University, Egypt
[3] Chief Engineer, Risk Management Solutions, Inc. 7015 Gateway Blvd, Newark, CA 94560

FIRE FOLLOWING EARTHQUAKE SIMULATION

The region under investigation is divided into small grid cells and described in terms of building density, construction type, fire break dimensions (street width), fire suppression capability and water availability. These quantities are assumed to be constant within a grid cell. The simulation starts with the estimation of the ground shaking throughout the region and the resulting shake damage to buildings and other structures. The number of ignitions is estimated from the earthquake intensity and the building stock distribution. The locations of the ignitions are selected randomly across the area with higher probability of ignition attributed to more densely populated areas. Fire stations respond by dispatching fire engines to suppress the ignitions. Engines are assigned to the fire closest to their station and a single engine is at first dispatched to each fire. If the fire engines required outnumbers the fire engines available, some ignitions conflagrate. At each time step the methodology checks the status of each fire and updates its dimensions according to the fire spreading model. After controlling a fire, engines are reassigned to the next closest fire. Considerations are given to building fire protection deterioration due to shaking. Water supply degradation is estimated based on the level of ground motion and liquefaction potential. Fires are tracked in the simulation as they expand until they are contained by the fire fighting personnel or are confined between fire breaks.

Data Requirements

The preparation of the input data to the simulation program requires a significant effort and relies heavily on the compilation of census data, commercial and industrial data, land use land cover maps, aerial photographs, city maps and the like. The area of interest is divided into a grid of variable resolution to optimize storage space. The exposure, fire spread simulation and results can be estimated at different grid resolutions. Figure 1 presents the 0.01 degree (approximately 1 km) cells for the San Francisco Bay area. The analysis could be carried out at an even finer resolution. In each cell, the building stock (exposure) is broken down by line of business and construction material and the total square footage is determined to estimate the number of ignitions following an earthquake. The footprint area occupied by each class of buildings is then calculated to determine the cell builtupness (ratio of area occupied by buildings to the total area of the cell). As an example, Figure 2 presents the builtupness for the Los Angeles region.

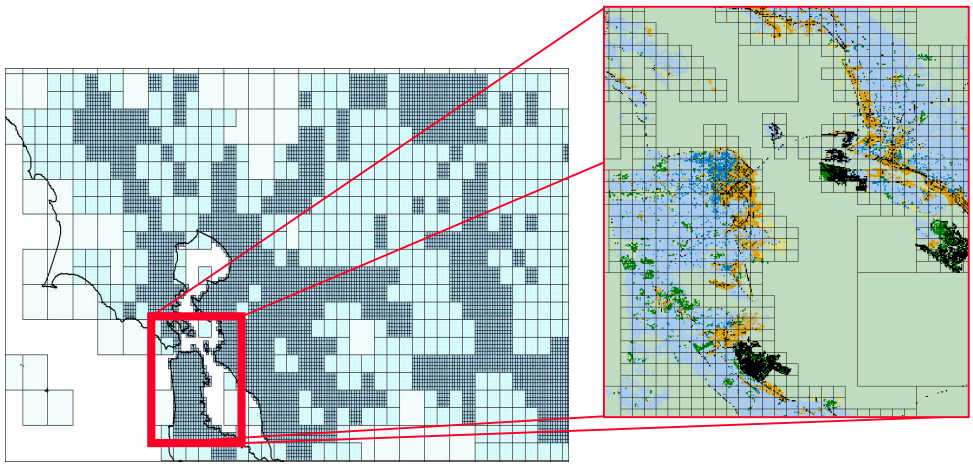

Figure 1: Discretized cells in the San Francisco Bay area.

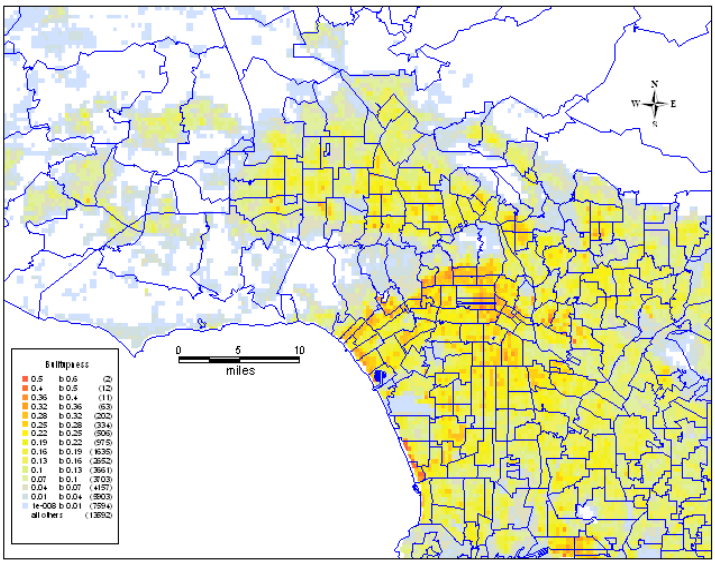

Figure 2: Builtupness for Los Angeles region.

The next step consists of spatially distributing the exposure. Major thoroughfares are explicitly modeled. For regular streets, an average block size and street width are used. Average building size and distance between buildings is then determined. Finally, the fire stations together with the number of fire engines are identified. This basic information is necessary for the simulation methodology to follow the evolution of the three phases of a fire: ignition, spread and suppression. The following sections present the details of the three modules.

Ignition

The ignition module estimates the number of fires expected to occur depending on the earthquake severity. The term "ignitions" refers to fires that ultimately require fire department response. Thus fires that are put out by the occupants of a building without the intervention of the fire department are not considered in this model. These fires are usually discovered very early and are put out before they can do substantial damage. These ignitions do not lead to significant losses.

The most common sources of ignitions include:

- Toppling over of unanchored items causing short circuits or fuel spills.
- Breakage of underground utilities (such as gas lines) that provides a fuel source for the ignition.
- Inter-story drift of structures, which may cause short circuits in electrical wiring.

The number of ignitions is a function of the following parameters:

- The level of ground shaking: peak ground acceleration (PGA) or intensity (MMI) at the site. This is the most important factor since an increase in the level of ground shaking results in a significant increase in the probability of utility line breakage and short circuits.
- The occupancy type of the building: residential, commercial, or industrial. The occupancy type determines the building contents, type of use, and usage hours. Commercial buildings for example are used more during the day than during the night. Residential buildings on the other hand are used more at night. Thus commercial buildings will have a higher ignition rate than residential buildings during daytime.
- The structure material, in particular: wood structures vs. non-wood structures. A spark from a short circuit more likely turns into a fire in a wood building than in a non-wood building, resulting in higher ignition rates for wood construction.

- Time of day. During meal times, more electrical and gas appliances are in use. This increases the potential for ignitions as compared to nighttime. Similarly, time of year is important in that gas or oil appliances are used in the winter for home heating.

Figure 3 presents a typical set of ignition curves used in the present study. Six similar sets of curves are used in the model to estimate the number of ignitions as a function of the following occupancies and building materials: residential wood and non-wood buildings, commercial wood and non-wood buildings and industrial wood and non-wood buildings. These curves were calibrated on five recent US earthquakes: San Fernando (1971), Morgan Hill (1984), Whittier (1987), Loma Prieta (1989) and Northridge (1994).

The ignition curves give the number of ignitions per unit area of building inventory as a function of PGA, in gals (cm/sec^2). The four ignition curves in Figure 3 represent the variation in the number of ignitions for earthquakes occurring at different times of day and different seasons. The four ignition curves correspond to earthquakes occurring in summer day time, summer evening time, winter day time, and winter evening time. Summer, winter, day, and evening are all considered as fuzzy variables with fuzzy weights shown in Figure 4 and Figure 5. Combining the membership functions in Figure 4 and Figure 5, the membership surfaces for summer day, summer evening, winter day and winter evening is derived. Typical summer evening fuzzy weights are shown in Figure 6.

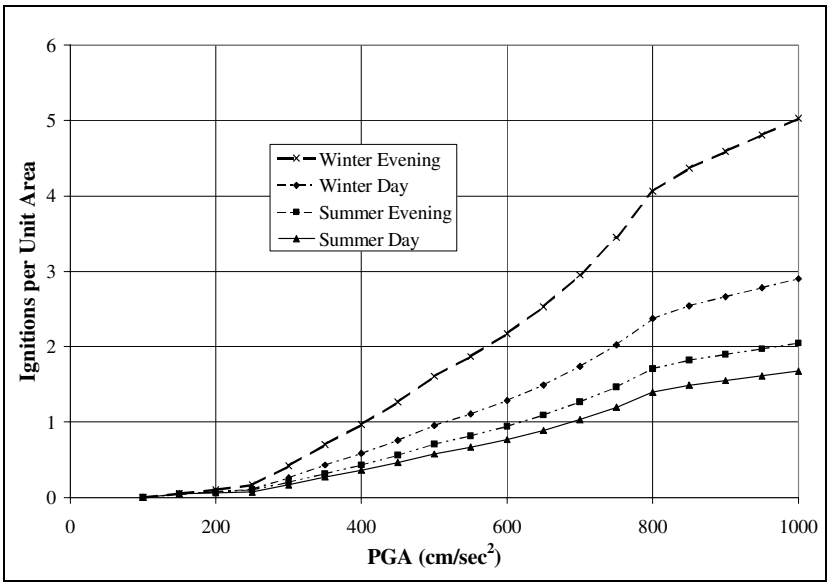

Figure 3: Typical ignition curves.

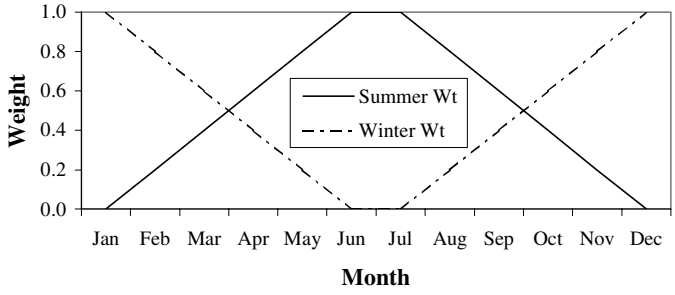

Figure 4: Fuzzy weights for different seasons.

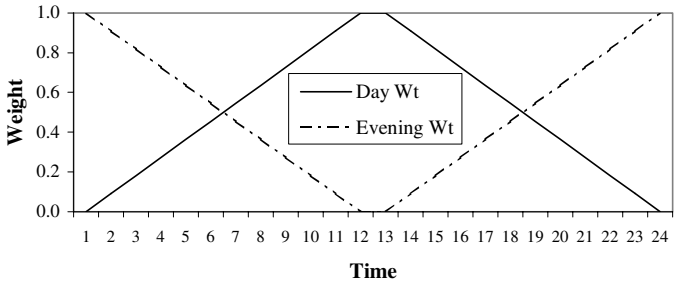

Figure 5: Fuzzy weights for different times of day.

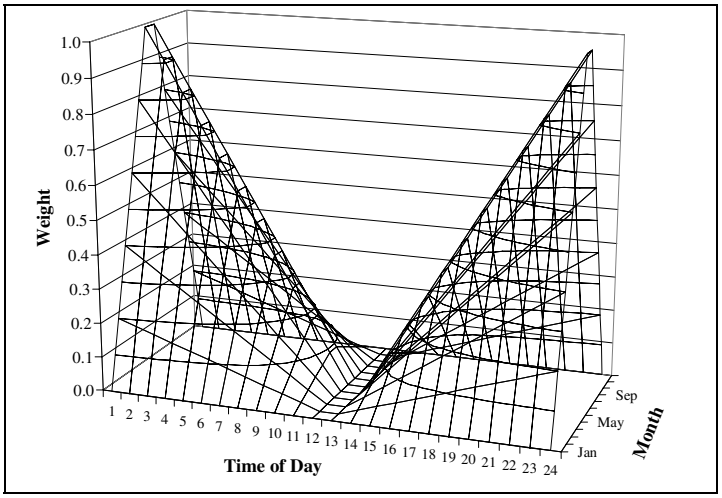

Figure 6: Fuzzy weights for summer evenings.

The number of ignitions for an earthquake occurring on a certain date and time of day is obtained by first calculating the membership value of the time and season of the earthquake from each of the summer day, summer evening (Figure 6), winter day, and winter evening surfaces. These four weights are used to obtain a weighted average of the number of ignitions from the four curves corresponding to the occupancy and structure type of the building.

The number of ignitions estimated using the above ignition model includes both fires starting immediately after the earthquake and those starting some time after the earthquake. Based on the empirical record, it is estimated that about 70 % of all fire ignitions start within a few minutes after the earthquake occurrence. The remaining ignitions start some time after the earthquake, ranging from an hour to possibly a day or so after the earthquake. A typical cause of these later ignitions is the restoration of electric power. When power is restored, short circuits that occurred due to the earthquake become energized and can ignite fires.

Fire Spread

The fire spreading model determines the fire spreading speed in four directions at each time step throughout the simulation: downwind, upwind and the two directions across wind. The fire spreading model used in the present study is based on the Tosho model developed by the Tokyo Fire Department in

Japan in 1997 [1]. This model is applicable to the U.S. since it requires a specific description of the type of exposure at risk. For the sake of completeness, it is presented in some detail.

Based on the Tosho Model, the fire spreading speed, $V(t)$, at any time, t, after the initial ignition is determined from:

$$V(t) = \frac{V_f}{1 + \{1.3 - 0.3\exp(-0.3t)\}\{(V_f / V_0 - 1\}\exp[-\{0.5V_f /(V_f - V_0)\}t]}$$

where:

V_o is the initial fire spreading speed in (m/h), at the startup time of the ignition

V_f is the final fire spreading speed in (m/h),

The initial fire spreading speed, V_o , is computed from:

$$V_0 = \delta \cdot g(h) \cdot (1 - c')$$

where:

$$\delta = \frac{\frac{\{r(U)a(a'V_w + b'V_m) + (a+2.6)d'Vc\}}{(a'+b'+d')} + \frac{r(U)\{d(a'+b')^2 V_{nn} + (d-1.3)(a'+b')d'(V_{nc} + V_{cn}) + (d-2.6)d'^2 V_{cc}\}}{(a'+b'+d')^2}}{a+d}$$

where:

a : length of one side of a building in meters

d : spacing between buildings (door to door) in meters

a' : the ratio of non-damaged bare wood structures

b' : the ratio of non-damaged fire resistive structures

c' : the ratio of fire resistive structures

d' : the ratio of totally damaged wooden structure

U : wind speed in m/sec

h : humidity in %

$r(U)$: factor depending on wind speed, U, and is equal to
$r(U) = 0.048U + 0.822$

$g(h)$: factor depending on humidity, h, and is equal to
$g(h) = -0.005h + 1.371$

V_w : fire speed inside wood buildings

V_m : fire speed inside fire resistive buildings

V_c : fire speed inside collapsed buildings and is equal to
$V_c = 98./(1.+3.9 \exp(-.094\ U^2))$ (m/h)

V_{nn} : fire speed from non-collapsed to non-collapsed buildings

V_{nc} : fire speed from non-collapsed to collapsed buildings

V_{cn}: fire speed from collapsed to non-collapsed buildings

V_{cc} : fire speed from collapsed to collapsed buildings

The final fire spreading speed, V_f , is computed from:

$$V_f = \frac{V_u + \exp\{-50(k - 0.14)\}V_1}{1 + \exp(\{-50(k - 0.14)\})}$$

where:

k : coefficient that performs a smooth transition for V_f from V_1 for small values of k (< 0.14) to V_u for high values of k (>> 0.14) and is calculated from
$k = (1\text{-}c')(a" + 0.85b")\ \{m(1\text{-}x)\text{-}0.1\}^{1.2}(U\text{-}4.9\text{-}8x)^{0.33}$

m : Builtupness, building density ratio, or building coverage ratio

x : total damaged ratio of wooden structures

$$x = \frac{d'}{a'+b'+d'} = \frac{0.54}{1+680\exp(-0.10\alpha)} - 0.0024$$

α : acceleration in gal

$a'' = a' + 0.0018 b' \alpha$ if $b' - 0.0018 b' \alpha < 0$ then $a'' = a' + b'$

$b'' = b' - 0.0018 b' \alpha$ if $b' - 0.0018 b' \alpha < 0$ then $b'' = 0$

however, if $m(1\text{-}x)\text{-}0.1 < 0$ or $U\text{-}4.9\text{-}8x < 0$ then $k = 0$

V_1 : fire spreading speed influenced by radiation

$$V_1 = (1-x)^2 [6 a_u V_o (m^{1.5} - m^2) + b_1](1-c')(a''+.85b'')(0.1U + 0.1)^{0.5} + V_o$$

$$a_1 = 0.31/m + 0.52$$

$$b_1 = (-0.1U - 1.8)/m + 2.7$$

V_u : fire spreading speed influenced by wind speed and temperature

$$V_u = 0.46(1-x)^2 [a_u V_o \{(1-c')(a''+.85b'') + 1.6((1-c')(a''+.85b''))^{-0.5}(U+0.1)^{-0.4}\} + b_u] m^{0.2} + V_o$$

$$a_u = \{1.4(U+1.0)^{-0.61} + 0.47\}/m + (4.4U^{0.19}) - 5.6$$

$$b_u = \{-8.9U^{0.75} - 8.6\}/m + (0.041U^{3.1}) + 49$$

It is assumed that an urban area is represented by a series of equal square (plan area) structures of average dimension a_o and with equal spacing between structures d. It is also assumed that the structures are arranged into city blocks. Each city block has an average dimension b_w and an average block separation (also referred to as fire break width) f_b.

The builtupness, m, differentiates between densely and sparsely populated areas. A value of builtupness equal to 0.35 represents a densely built area, while a value of 0.10 represents an area which is not very densely built. The builtupness, m, is computed from the

$$m = \left[\frac{{b_w}^2}{(b_w + f_b)^2}\right]\left[\frac{{a_o}^2}{(a_o + d)^2}\right]$$

where:

a_o : average building dimension
d : average distance between buildings
b_w : average block width
f_b : fire break width

The fire is assumed to spread in an oval shape, through an evenly distributed fuel load, with the longer axis in the wind direction, as shown in Figure 7. In an actual urban conflagration, fires exhibit this trend initially, but the final shape of the fire spread differs, as different fuel loads are experienced, fires merge, and different fire suppression actions take place. At each time step the fire dimensions in the downwind direction K_d, the upwind direction K_u and the side wind direction K_s are updated by using the present fire spreading speeds.

The fire spreading speed differs in the downwind direction, from both the upwind and side wind directions due to the difference in wind speed. The actual wind speed is used in computing the fire speed in the downwind direction, while zero wind speed is used in computing the fire speed in both the upwind and sidewind directions.

The fire burnt area at any time step is computed by calculating the area of the fire ellipse as follows:

$$\text{Fire Area} = \pi\left(\frac{K_d + K_u}{2}\right)K_s$$

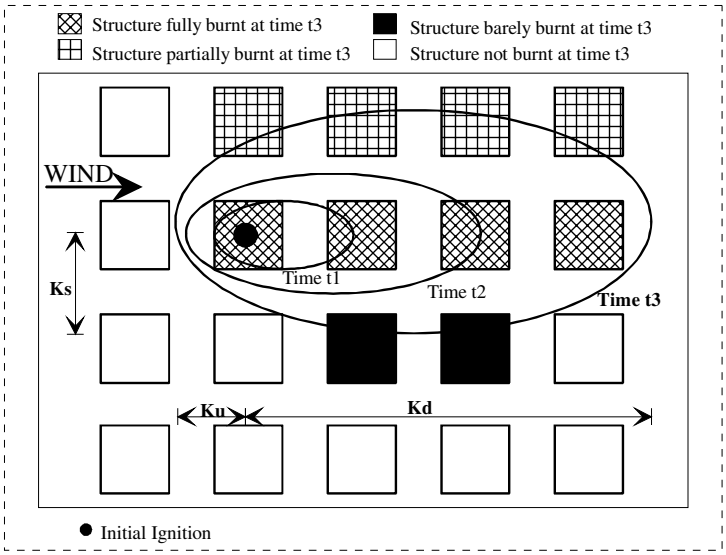

Figure 7: Process of fire spread.

Comparison of the Tosho Model with the Hamada Model.

Before the Tosho model was introduced, the Hamada Model [2] was the most commonly used model for fire spread. The Hamada model has been criticized for its high fire spreading speed, which leads to higher losses than experienced in historical events. One of the reasons was that the Hamada model had been conservatively calibrated for wood structures only. Figure 8 presents a comparison of the fire spreading speed estimated by the Hamada and the Tosho models. One notes that:

- The Tosho spreading speeds are always less than the Hamada fire spreading speeds.
- At zero wind speed, the Tosho fire speeds are one half the Hamada fire spreading speeds.
- At higher wind speeds the Tosho fire speeds are about 20 to 30 percent those of the Hamada model.

These decreases reflect a more realistic processing of recent data such as the 1995 Kobe earthquake.

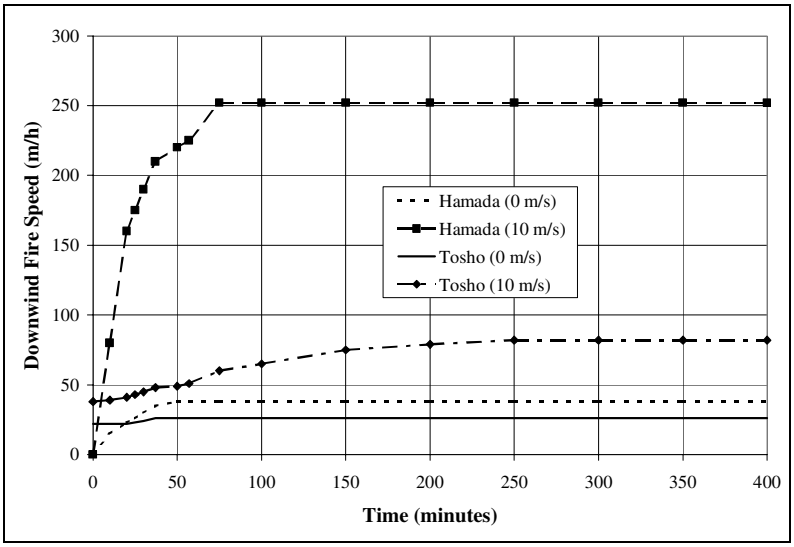

Figure 8: Comparison of the Tosho and Hamada models.

Suppression

The term suppression is defined as the effort required to fight a fire, beginning with its discovery. The steps of the suppression activity are defined as the discovery and report time, the engine travel time and the control time. The discovery and report time is the elapsed time from the start of the fire until it is reported to the fire agency. The arrival time is the time taken for the fire suppression personnel and equipment to arrive at a fire location. After an earthquake, it is expected that fire engines will travel at slow speed due to damage to the road network, debris in the streets, etc. The time and resources needed to control a fire depend upon the status of the fire as the first engine reaches the site. Since the status of a fire varies over time, the model continuously updates the fire status and resource requirements.

Suppression Capability

Much of the suppression module is based on the Hazus methodology [3] and will simply be summarized herein for completeness. The minimum number of engines needed to suppress a fire is first estimated based on the size and type of fire. The amount of water required is estimated in terms of water flow and flow duration and is function of the size of the fire and the wind velocity. For each fire, at each time step of the analysis, the model checks the available water flow and the number of engines at the scene and compares them to the number of engines and amount of water required to control the fire to determine the fire suppression effectiveness. The fire suppression effectiveness is used to modify the rate of fire spread.

Fire Spread at Natural Fire Breaks

Fire breaks are one of the ways to stop fires from spreading. Fire breaks abound in an urban area and include streets, highways, parks, and lakes. The model accounts for fire breaks as follows:

- Fires spread within a city block is modified by the fire suppression effectiveness when the fire is attended. The model keeps track of the spread.
- When a fire reaches a fire-break, the model calculates the probability that the fire is stopped at the fire break. As shown in Figure 9, the probability of a fire crossing a fire-break increases with the wind velocity, decreases with the width of the fire break, and decreases with the presence of active fire suppression. It can be seen that wind speed and the presence of fire suppression play an important role. These curves are based on studies by Dames and Moore [4].

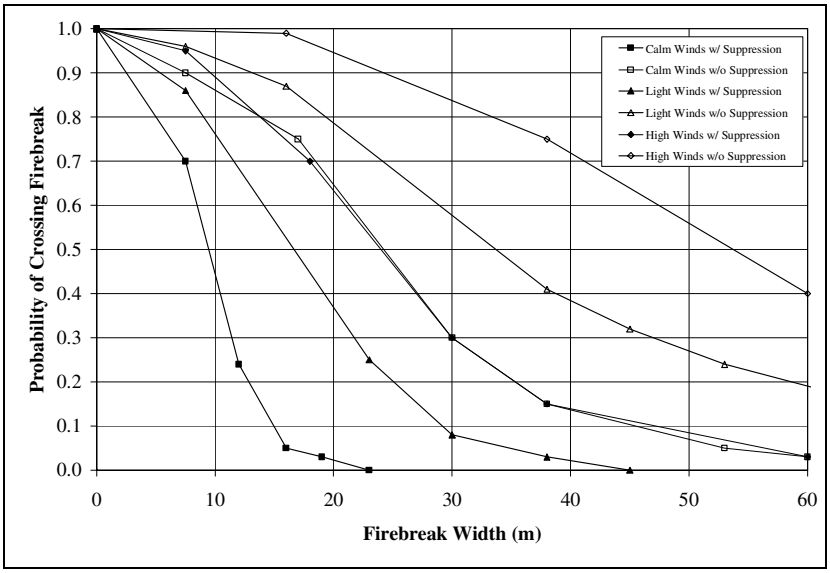

Figure 9: Probability of firebreak crossing.

RESULTS

Figure 10 presents the simulation status some time after the occurrence of a repeat of the 1906 earthquake in San Francisco. The small buildings indicate the location of the fire stations, the dots are the locations of the fires, and the lines with the truck show how the fire engines have been dispatched from the station to the fire. It can be noted that the engines move in a straight line from the station to the fires (city streets are not modeled to calculate engines travel time). The wind speed is constant over the duration of the simulation and is 10 km/h in this simulation. Figure 11 presents the status of the fires at the same simulation time as Figure 10. The ellipses indicate the burnt area, the gray ellipses represent fires that have been brought under control while the red ones are still burning uncontrolled. The simulation ends when all the fires are either brought under control or are stopped by fire-breaks and run out of fuel.

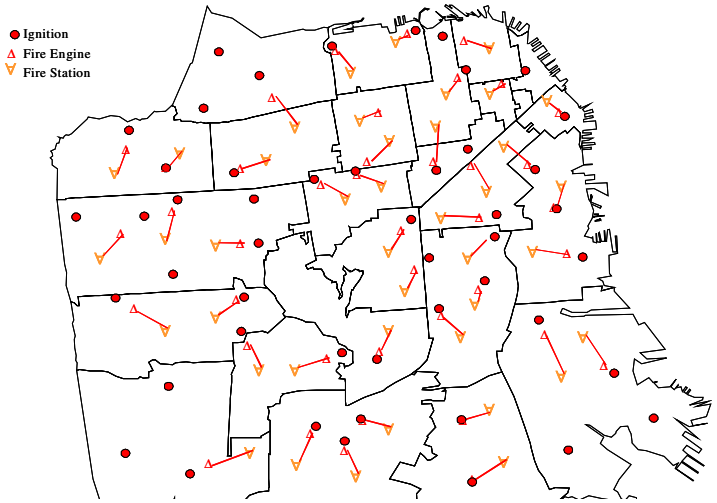

Figure 10: Ignition and deployment of fire engines.

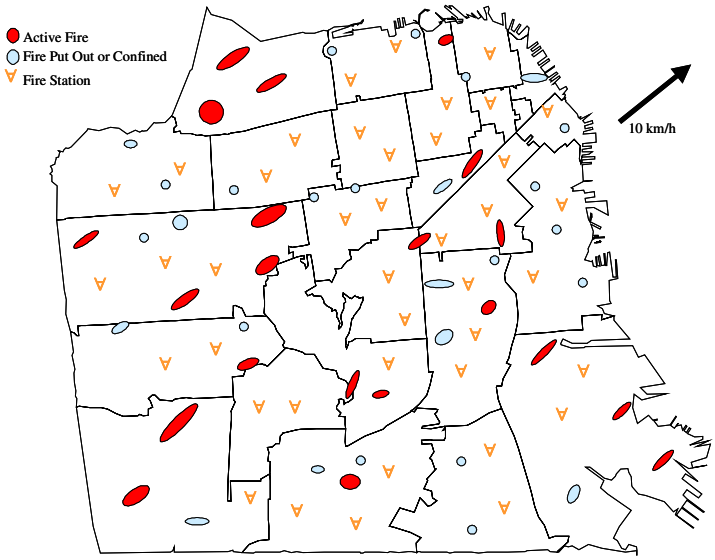

Figure 11: Active and controlled fires in a simulation.

Figure 12 presents a measure of the ground shaking for a repeat of the 1906 event. A grid has been overlaid over the city and all the parameters are assumed constant within a cell. For this study the size of the cell is 0.01 x 0.01 degree (about 1km x 1km). The level of shaking is quantified in terms of peak ground acceleration (gals or cm/sec^2). The PGA does not always show a uniform decay as the distance from the fault increases because the acceleration is affected by the local soil condition. Figure 13 presents the mean burnt area within each cell at the end of a large number of simulations. By overlaying the exposure in each cell with the burned area one can determine the expected fire loss in each cell and for the whole area. Figure 14 and Figure 15 present the same information for the Seattle area. The scenario event considered is an earthquake of magnitude 7.0 on the Seattle fault. The accelerations for this event are comparable to the accelerations generated in San Francisco by the 1906 earthquake, however the fire losses are much lower because the builtupness is significantly lower in Seattle than in San Francisco.

When comparing the burnt area between simulations, it is not uncommon to find the worst case scenario to be twenty times larger than the most optimistic scenario. Of course, these extreme scenarios have a very low probability of occurrence as compared to the average scenarios. The most sensitive parameters are the number of fires, the wind speed and the location of fires.

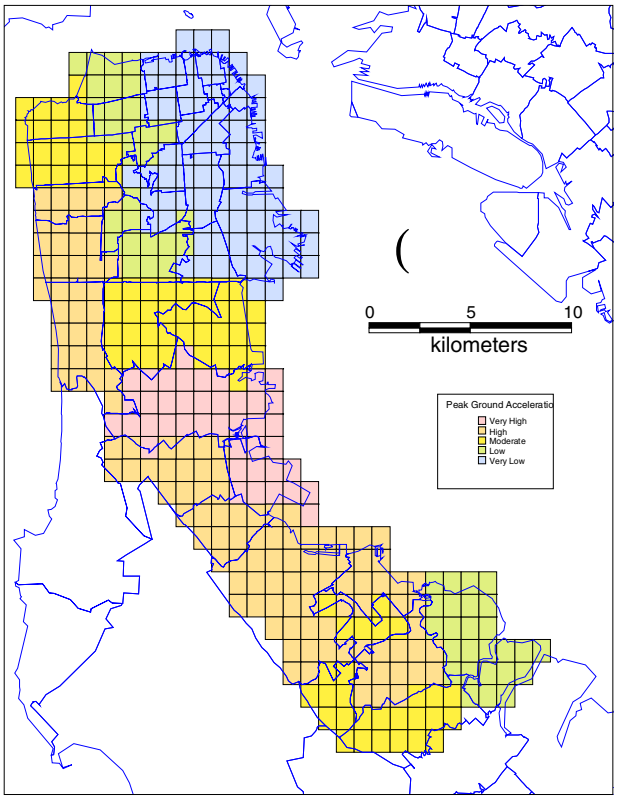

Figure 12: Peak ground acceleration for the scenario event in San Francisco.

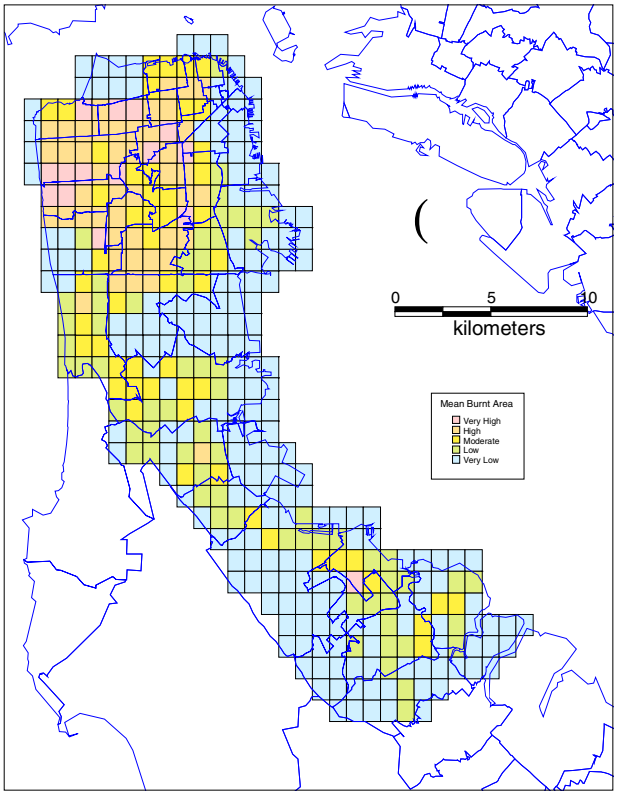

Figure 13: Mean burnt area for the scenario event in San Francisco.

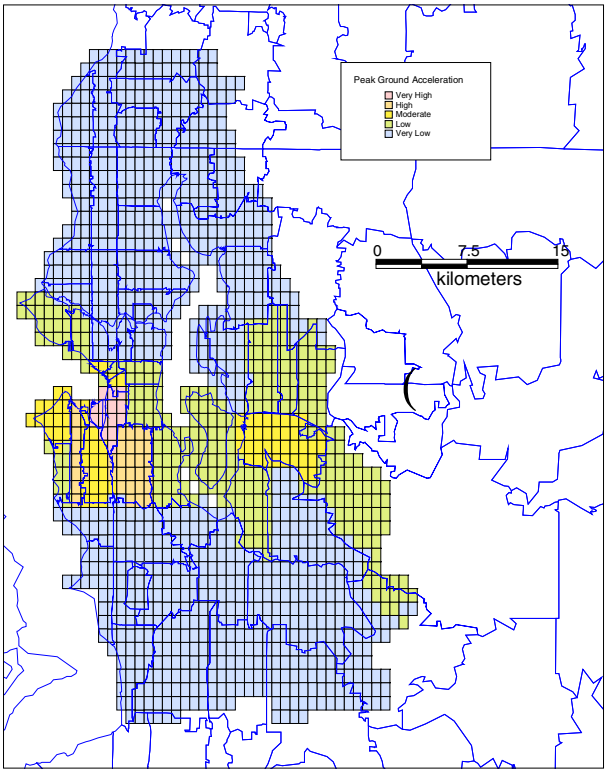

Figure 14: Peak ground acceleration for the scenario event in Seattle.

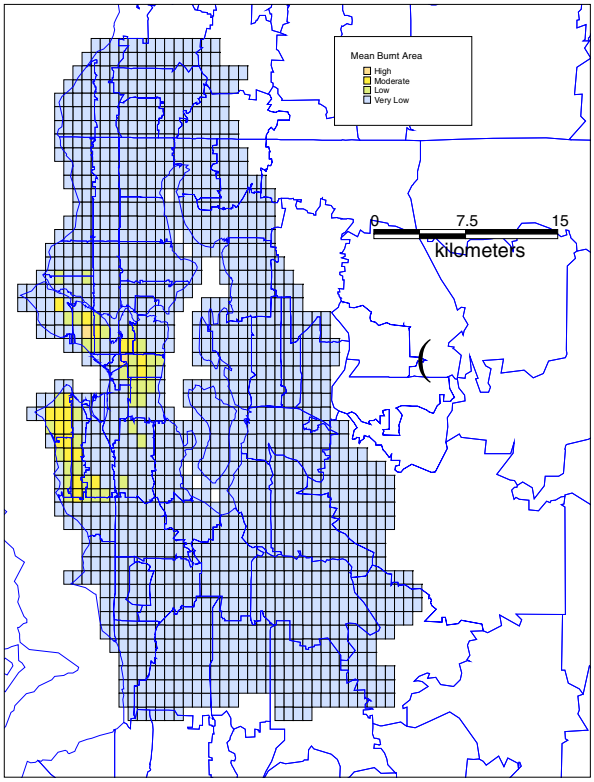

Figure 15: Mean burnt area for the scenario event in Seattle.

When simulating an historical event, a large amount of uncertainty is removed by fixing the time of the day and time of the year, thus reducing significantly the uncertainty around the number of ignitions. Similarly by fixing the wind speed, the fire spread model's behavior is more constrained. Simulations still need be done to cover the uncertainty on number and location of fires, engine assignment, etc. Figure 16 presents the mean burnt area estimated for a repeat of the Northridge (1994) event compared to the location of reported fires in 1994. The high level of correlation gives confidence that the simulation methodology generates realistic results.

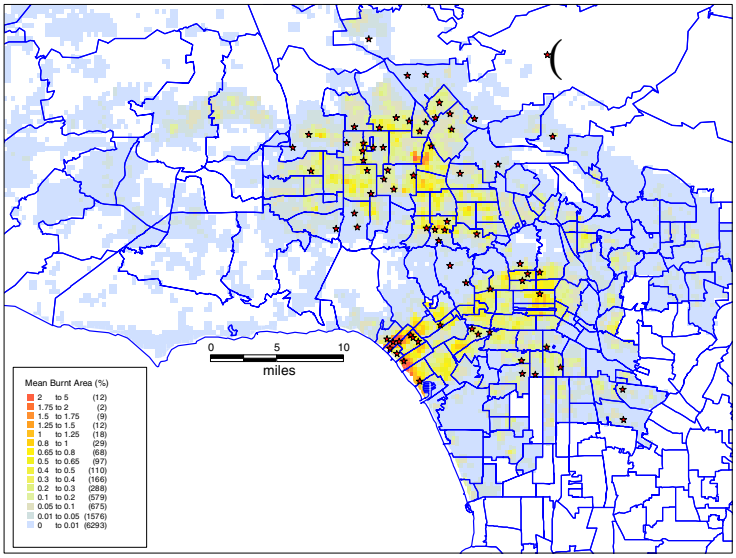

Figure 16: Estimated mean burnt area and reported fires in the Northridge event.

CONCLUSIONS

The simulation methodology described in this paper estimates post earthquake fire losses in the U.S. The main parameters leading to conflagration are modeled together with their uncertainty. Numerous simulations are performed to capture the range of possible losses and their associated probabilities. The large uncertainty reflected in the results is an inherent characteristic of the randomness of fire following earthquakes.

REFERENCES

1. Tokyo Fire Department, "Determination and Measures on the Causes of New Fire Occurrence and Properties of Fire Spreading based on an Earthquake with a Vertical Shock", Fire Prevention Deliberation Council Report, Page 42, March 1997.
2. Hamada, M., 1975. "Architectural Fire Resistant Themes", No.21, Kenchikugaku Taikei, Shokokusha, Tokyo.
3. HAZUS, Earthquake Loss Estimation Methodology, Technical Manual, Volume III, prepared by the National Institute of Building Sciences, for the Federal Emergency Management Agency, 1995.
4. Dames and Moore Report, March 1987. "Fire Following Earthquake, Estimates of the Conflagration Risk to Insured Property in Greater Los Angeles and San Francisco," Report to All-Industry Research Advisory Council, C. Scawthorn.